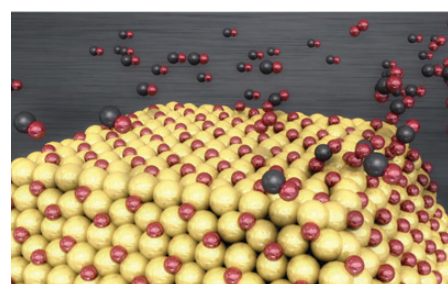
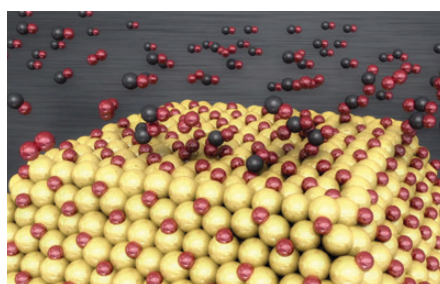
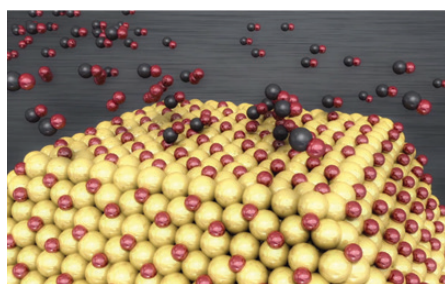
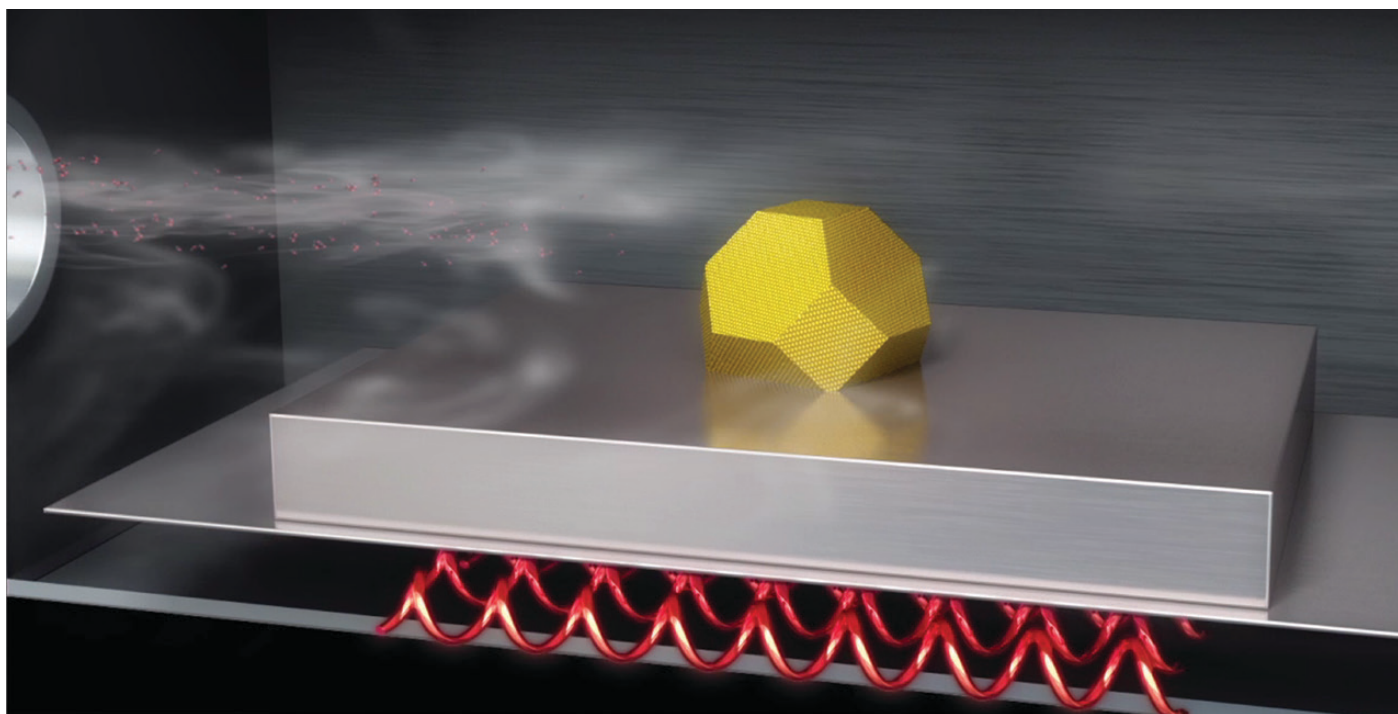


# Environmental Transmission Electron Microscopy

*In situ* characterization application examples in  
heterogeneous catalysis research



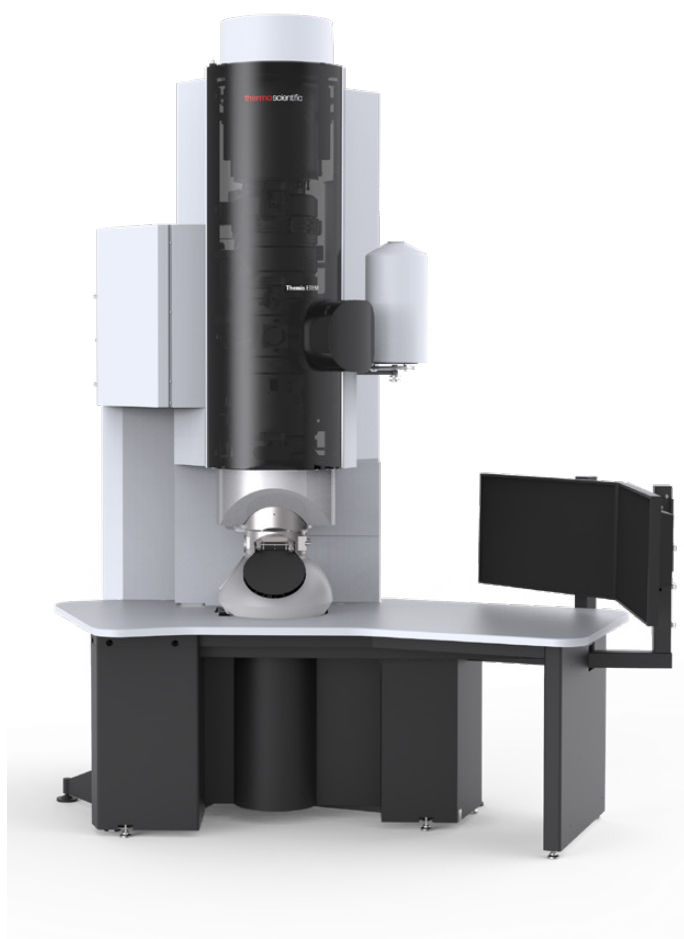
The continuing dependence on non-renewable fossil fuels, as well as the demand for new unconventional renewable fuel and feedstock resources for energy, transportation and industry, requires a continuing effort in materials research, particularly catalysis research, at the nanoscale.

As part of this research, it is necessary to characterize existing functional nanomaterials or apply rational design strategies to new catalysts. This requires a detailed understanding of structure-performance relationships and atomic-scale insight into the geometric and electronic structure, and chemical composition. Transmission Electron Microscopy (TEM) is often used for these applications, but the instruments have required significant modification in order to be safely used for catalysis research.

### Themis ETEM

The Thermo Scientific™ Themis™ ETEM is the dedicated atomic-resolution Scanning/Transmission Electron Microscope (S/TEM) solution for time-resolved studies of the behavior of nanomaterials during exposure to reactive gas environments and elevated temperatures. Designed specifically for *in situ* dynamic experiments in catalysis, Themis ETEM features a unique, innovative differentially pumped objective lens for window-free imaging, and gas inlets for safe application of inert and reactive gas.

Gas pressures in ETEM experiments can be accurately preset from  $10^{-3}$  Pa up to 2000 Pa (for  $N_2$ ). The new software-controls offer a range of settings to accommodate both handling by novice (automatic mode) as well as advanced (manual control) operators. The ETEM is equipped with a mass spectrometer for determining gas composition in either the gas inlet system or the specimen area. A built-in plasma cleaner allows for cleaning of the specimen area after using a gas. In addition, compatibility with regular Themis TEM holders for easy sample insertion, and space for full double tilt capability for applications like 3D tomography further extend the functionality of the ETEM to other materials



### Key Benefits

**Observe** functional nanomaterials' time-resolved (dynamic) response to gas and temperature stimuli

**Study** gas-solid interactions at the nanometer and atomic scale, including shape and morphology, and interaction at surfaces and interfaces

**Gain insight** at the atomic-scale into the geometric and electronic structure, and chemical composition of functional nanomaterials

## Nanoparticle size, shape and structure: visualize nanocatalysts in operando

Catalysis is the change in rate of a chemical reaction due to the participation of a substance called a catalyst. Unlike other reagents that participate in the chemical reaction, a catalyst is not consumed by the reaction itself. A catalyst may participate in multiple chemical transformations.

In general, catalysts positively influence a chemical process to achieve a higher selectivity, a higher yield, or fewer amounts of side products while consuming less energy. Some examples of catalyst and support materials are metals, metal oxides, and zeolites.

Substances that slow a catalyst's effect in a chemical reaction are called inhibitors. Substances that increase the activity of catalysts are called promoters, and substances that deactivate catalysts are called catalytic poisons.

Nearly 90% of all chemical processes use catalysts; therefore, it is indispensable to develop a fundamental understanding of the functionality of catalysts.

The catalytic activity of catalysts seems to, among other influences, depend strongly on their size, shape, and structure. While *ex situ* characterization offers important insight to the catalyst's structure and composition, this observation might not provide the information about changes to the catalyst's structure and properties while in its operating state. This is fundamental to describing the catalyst's structure – property relationships because in operando, the catalyst undergoes significant changes in size, shape, structure and composition to become active (see Figures 1 & 2).

For this reason it is very important to obtain the structural information about the catalyst under reactive conditions, like elevated temperatures and pressures to understand and to improve the catalytic activity and functionality of new catalysts.

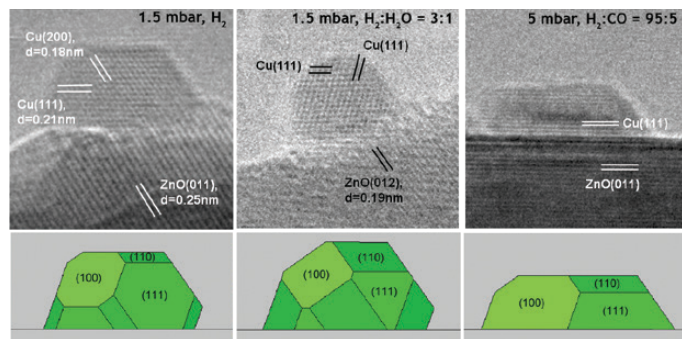


Figure 1. *In situ* HRTEM images of a methanol synthesis catalyst consisting of Cu nanocrystals on ZnO in various gas environments at a temperature of 220°C. Below the corresponding Wulff constructions of the Cu nanocrystals. The HRTEM images have been recorded *in situ* at a pressure of 1.5 mbar of H<sub>2</sub>; and at a total pressure of 1.5 mbar in a gas mixture of H<sub>2</sub>:H<sub>2</sub>O = 3:1; and at a total pressure of 5 mbar in a gas mixture of H<sub>2</sub> (95%) and CO (5%), respectively.

Ref. P. L. Hansen et. al., *Science* vol 295 (2002) 2053-2055

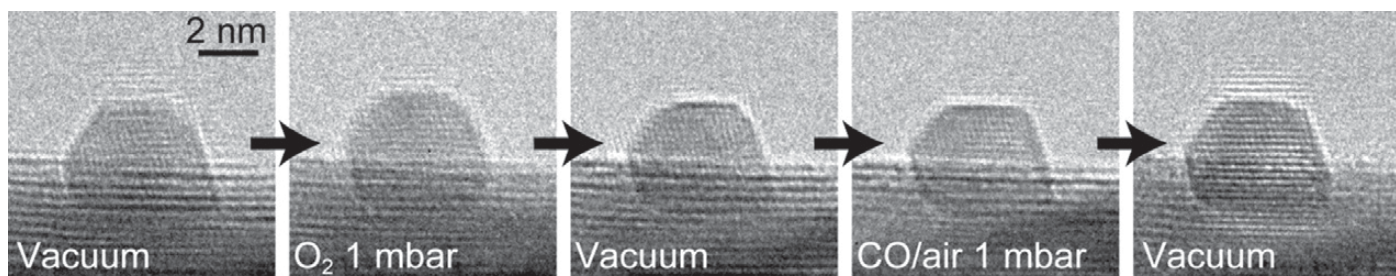
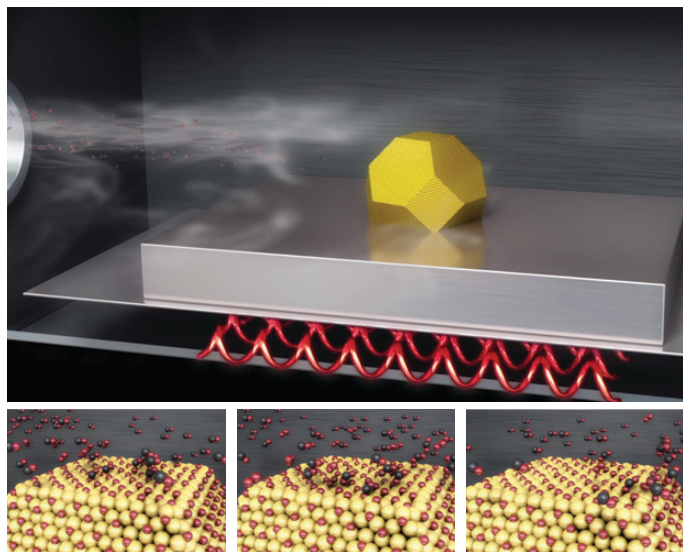


Figure 2. Reversible change in the morphology of a gold nanoparticle supported on CeO<sub>2</sub> between vacuum and gas environments (O<sub>2</sub> and 1 vol% CO/air gases). After introducing the O<sub>2</sub> gas in vacuum, the morphology of the gold nanoparticle changed from faceted to a roundish morphology. After removing the O<sub>2</sub> gas, the gold nanoparticle morphology reverted back to a faceted morphology.

Subsequently, 1 vol% CO/air was introduced under vacuum. The major {111} and {100} facets appeared clearly in 1 vol% CO/air. After removing 1 vol% CO/air, the morphology of the gold nanoparticle appeared to be faceted as in the proceeding observations in vacuum.

Ref. T. Uchiyama et. al., *Angew. Chem.* (2011), 123, 10339–10342

**NOTE:** Certain gases may be not approved for use with the ETEM or their use may be restricted. Please contact Thermo Fisher Scientific for additional information on approved gases and our gas approval process.

**Nanoparticle size, shape and structure:  
visualize nanocatalysts in operando**

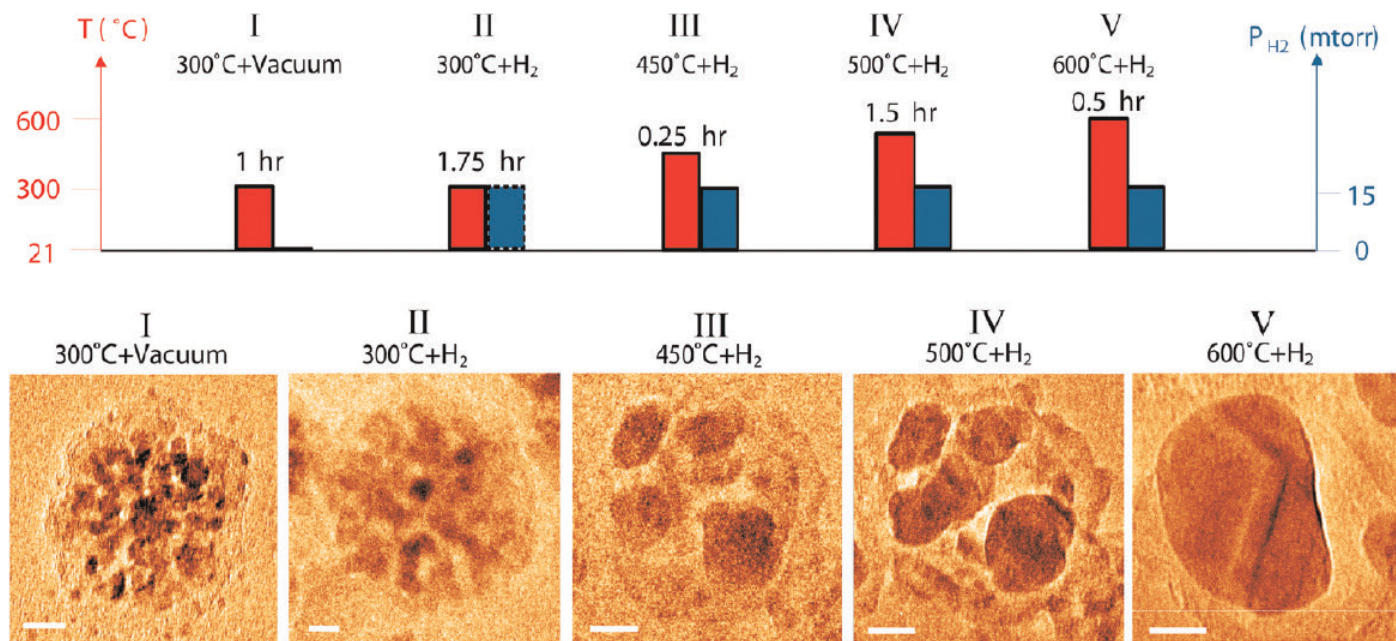


Figure 3. *In situ* observation of structural changes of Co/CoOX catalysts at different reduction conditions. Nanoporous cobalt/silica catalysts relevant to Fischer-Tropsch synthesis, an industrial reaction that converts syngas (mixture of hydrogen and carbon monoxide) to liquid fuels. (Upper image) Heating and H<sub>2</sub> gas environmental conditions and their durations. For a period of 30 minutes, the H<sub>2</sub> gas pressure was raised to ~6.5 Torr.

(Lower image) *In situ* ETEM images of the nanocomposites under the corresponding environmental treatments. Scale bars are 10nm. The CoOX reduction into metallic cobalt results in an increase of an effective particle size of the porous structure.

Ref. H. L. Xin et al., ACS Nano, 2012, 6 (5), pp 4241–4247, DOI: 10.1021/nn3007652

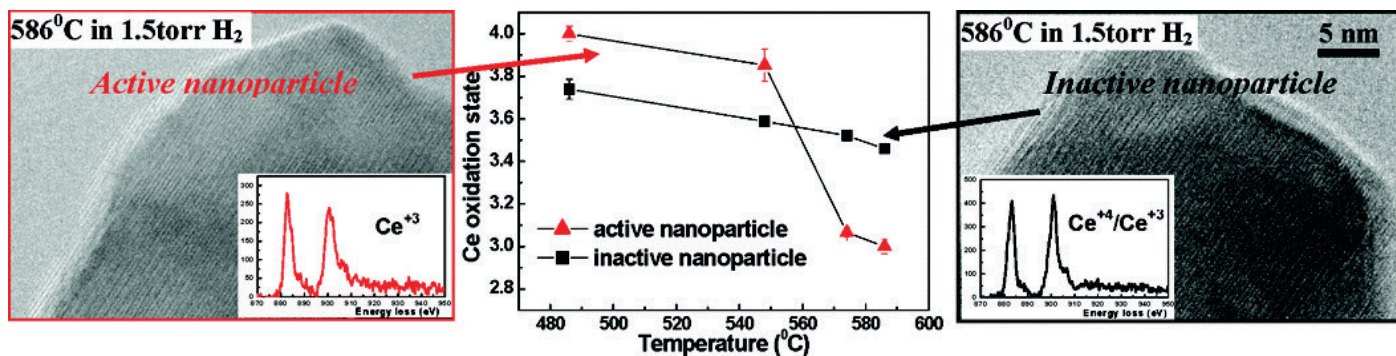


Figure 4. Nanoscale ceria zirconia particles are a critical component in the modern automotive three-way catalytic converter and have potential applications in other areas such as fuel cells, where redox functionality is important. *In situ* studies allow following the dynamic redox process taking place in individual ceria zirconia nanoparticles with changes in the oxygen chemical potential. Considerable variability in the redox activity have been observed with correlation of these differences to nanoscale structural and compositional measurements.

The more active structure has predominantly disordered cations and shows no evidence for oxygen vacancy ordering during reduction. (Left and right) *In situ* HRTEM observations from nominally identical ceria zirconia nanoparticles recorded at 586°C in 1.5 Torr of H<sub>2</sub>. The *in situ* EELS (insets) show that the particle on the right is more strongly reduced than the particle on the left. (Center) Oxidation state for same two particles as a function of temperature.

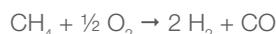
Ref. R. Wang, et al., Nano Lett., (2008) Vol. 8, No. 3, 962-967

## Production of syngas by partial oxidation of methane: Ni catalyst activation process

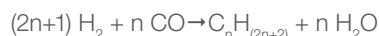
Synthesis gas (Syngas) is a mixture containing certain amounts of carbon monoxide (CO) and hydrogen (H<sub>2</sub>). Production methods are steam reforming of natural gas or liquid hydrocarbons, and the gasification of coal or biomass.

Syngas is used as intermediate in creating synthetic natural gas. The hydrogen in syngas is used in refinery and in fuel cells, and is the base for the production of ammonia (NH<sub>3</sub>). Syngas is an essential base product in the chemical industry and is used in the Fischer–Tropsch process to produce alkanes such as diesel fuel, synthetic petroleum, or is converted to methanol (CH<sub>3</sub>OH).

As an example, partial oxidation of methane (CH<sub>4</sub>) is an important reaction for the production of syngas:



Because of its slight exothermic nature, and the obtained product syngas ratio of H<sub>2</sub>:CO=2 is beneficial as input for Fischer–Tropsch synthesis:



The process of partial oxidation of methane may also be useful for other energy-related processes, such as fuel reforming for high-temperature fuel-cell applications.

Noble metals are very efficient and stable as catalysts for converting methane to syngas; however, noble metals are costly for large-scale applications. Supported Ni catalysts, as less expensive options, have shown high conversion efficiencies (see Figure 5) at low cost, although deactivation by coke formation and sintering can be problematic.

Figure 6 shows the development of the structure, composition and morphologies in model Ni/SiO<sub>2</sub> catalyst during ramp-up for partial oxidation of methane under high conversion conditions. The gas composition along the catalyst bed varied in space and time during ramp-up. Essentially there was no single “reactor condition” in this case and the variation in the gas composition had to be taken into account in the design of experiments so that the correct structure property relations could be determined.

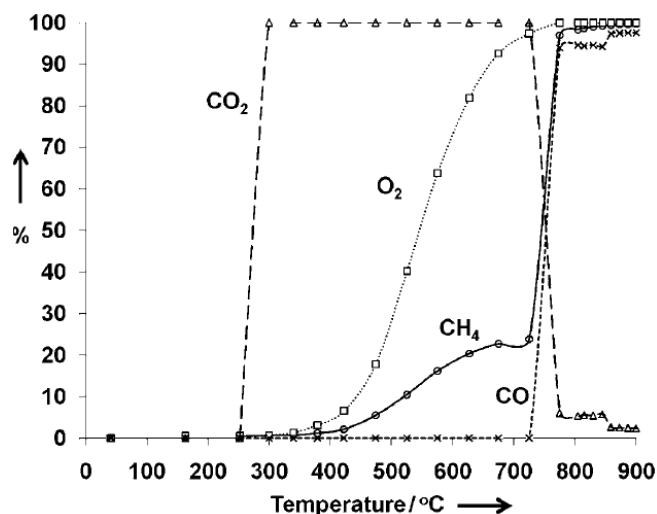


Figure 5. Conversion and selectivity for partial oxidation of methane over a model 2.5 wt% Ni/SiO<sub>2</sub> catalyst.

Ref. S. Chenna, R. Banerjee, and Peter A. Crozier, *ChemCatChem* (2011), 3, 1051 – 1059

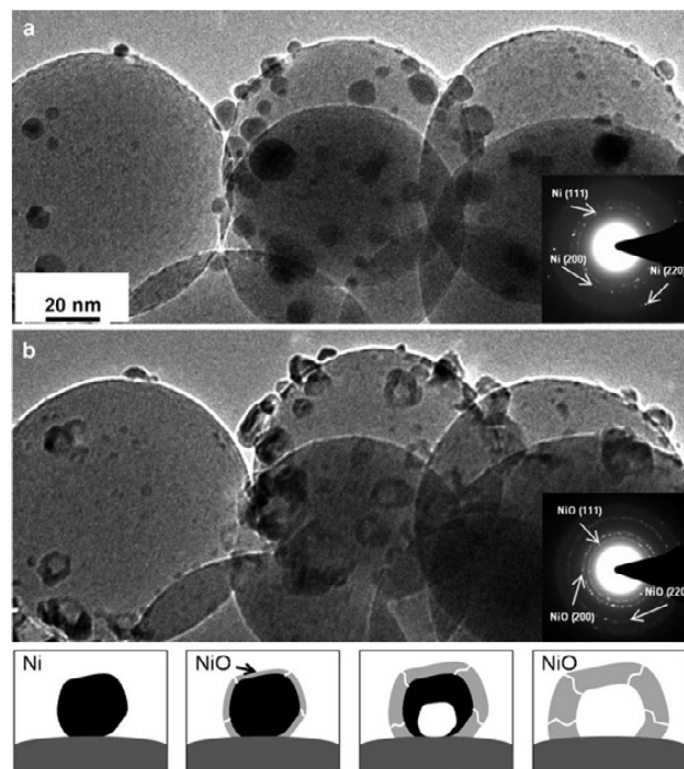


Figure 6. (Upper image) Partial oxidation of methane catalyst Ni/SiO<sub>2</sub> in presence of 1 mbar of H<sub>2</sub> at 400°C. (Middle image) same catalyst in presence of 1 mbar of mixture of CH<sub>4</sub> and O<sub>2</sub> in 2:1 ratio at 400°C.

(Lower image) Diagram of NiO void formation by Kirkendall effect.

Ref. S. Chenna, R. Banerjee, and Peter A. Crozier, *ChemCatChem* (2011), 3, 1051 – 1059

**NOTE:** Certain gases may be not approved for use with the ETEM or their use may be restricted. Please contact Thermo Fisher Scientific for additional information on approved gases and our gas approval process.

### Catalyst deactivation by carbonaceous layer growth

In a vast number of commercially relevant catalytically chemical processes, the deposition of coke (carbon) is a by-product of the underlying reactions. This causes catalyst deactivation and can lead to reduced process efficiency.

There is an ongoing interest in stabilizing the activity of supported catalytical nanoparticles and to understand the processes by which carbon-base layers, forms and accumulates on their surface.

### Natural gas conversion into synthesis gas: steam reforming catalyst Ni/MgAl<sub>2</sub>O<sub>4</sub>

Steam reforming is a fuel reforming process that produces hydrogen or other useful products from fossil fuel such as a natural gas, mainly methane CH<sub>4</sub>. As described previously, hydrogen is a renewable fuel source and an important reactant in a large number of chemical processes.

There is a tremendous research effort in designing affordable catalyst heterostructures. In addition to revealing the structure-function relationship, this research is leading to understanding and preventing catalyst deactivation that occurs when carbon-layer growth that covers the active sites. Direct visualization, such as *in situ* HRTEM, plays an essential role in this (see Figure 7).

### Alkane dehydrogenation: alkene producing catalyst Pt/MgO

Dehydrogenation is widely used for the transformation of alkanes (hydrocarbons with carbon-carbon single bond) to alkenes (olefins, carbon-carbon double bond). The simplest example of this reaction is the catalytic dehydrogenation of ethane to ethene:



The catalytic alkane dehydrogenation process has the advantages of a high selectivity of valuable alkenes and the formation of hydrogen as a by-product (see Figure 8). Alkenes are essential building blocks in the petrochemical industry. The C-C double bond in alkenes gives them the ability to undergo polymerization to form a huge variety of polymers (plastics). Alkenes are also an important starting material in organic synthesis, forming products such as alcohols, aldehydes, epoxide, or amines. All of these compounds/chemicals are the base for products such as adhesives, fertilizers, carpets and paints

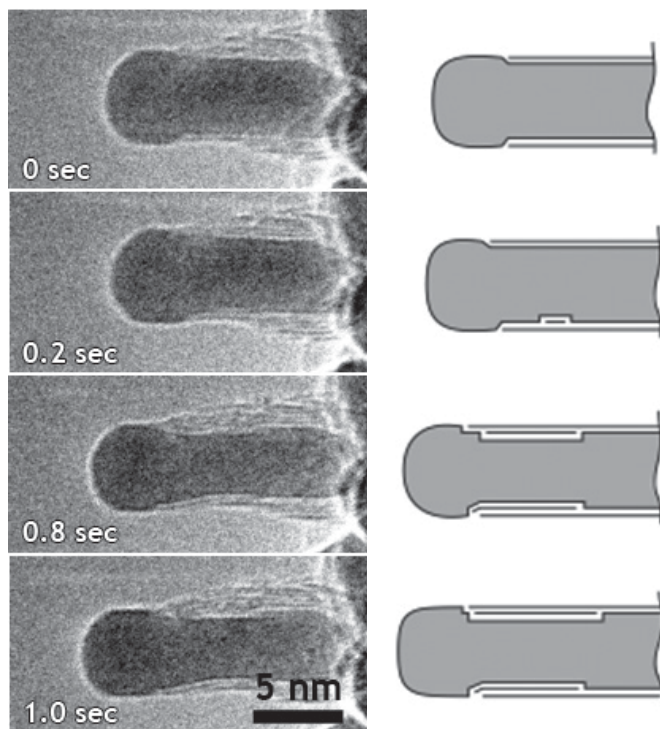


Figure 7. Carbon nanofiber growth by catalytic decomposition of methane over a catalyst consisting of Ni nanoclusters supported on MgAl<sub>2</sub>O<sub>4</sub>. Image sequence (Left) and drawings (Right) illustrate the positions and effect of mono-atomic Ni step edges at the C-Ni interface. Dynamic *in situ* ETEM study with CH<sub>4</sub>:H<sub>2</sub> = 1:1 at a total pressure of 2.1 mbar with the sample heated to 536°C.

Ref. S. Helveg, et. al., NATURE (2004) VOL 427, 426-429

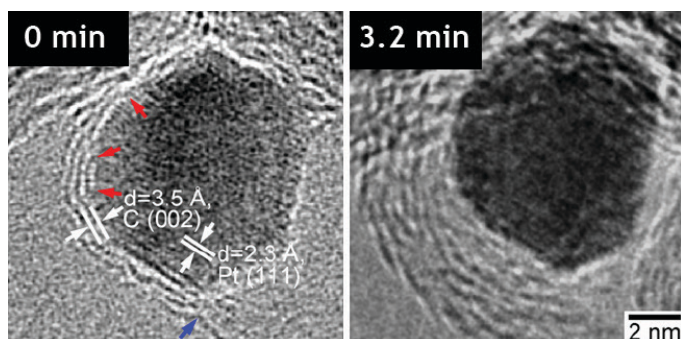


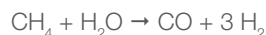
Figure 8. Dynamic *in situ* ETEM study (1.3 mbar C<sub>2</sub>H<sub>6</sub>, 475°C) with atomic-scale resolution Carbon layer growth during catalytic dehydrogenation over a catalyst consisting of Pt particles supported on MgO. Surface-step are identified as growth centers for graphene.

Ref. Zhenmeng Peng, et. al., Journal of Catalysis 286 (2012) 22–29

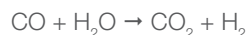
### Catalytic low temperature CO oxidation

Low temperature carbon monoxide (CO) oxidation is needed in various applications, such as in indoor air purification, safety devices (e.g., in laboratories using CO), submarine ventilation systems, and catalytic converters for cold-start emissions control of automotive exhausts. Another important application is the purification of hydrogen H<sub>2</sub>. H<sub>2</sub> gas is used in fuel cells. And H<sub>2</sub>-rich gas mixtures are an essential feedstock for chemical and energy-generating processes, including in petrochemical refineries and the production of chemicals (such as ammonia, methanol, etc.).

The H<sub>2</sub>-rich gas mixture obtained for instance by steam reforming of a hydrocarbon fuel:



usually contains by-products, mainly CO in the range of concentrations of typically ~1 vol%, even after the water-gas shift reaction:



Unfortunately this small amount of CO present in the reformed gas mixture poisons the active sites of a catalyst, for instance, the electrodes of a fuel cell. Among the many approaches selective catalytic oxidation ( $\text{CO} + \frac{1}{2} \text{O}_2 \rightarrow \text{CO}_2$ ) has been found to be the most effective way to remove the trace amount of CO from hydrogen. An efficient CO oxidation catalyst is thus necessary. It should be highly selective, because H<sub>2</sub> oxidation should be minimized, and the catalyst must be resistant to CO<sub>2</sub> and H<sub>2</sub>O deactivation. In ongoing research efforts, supported noble metal catalysts on transition metal oxides show interesting performances.

**Temperature dependence of CO conversion rate: catalyst for automobile exhaust gas treatment Pt/CeO<sub>2</sub>**  
Platinum (Pt) nanoparticles supported on CeO<sub>2</sub> (Pt/CeO<sub>2</sub>) are currently used as a component in three-way catalysts for automobile exhaust gas treatment and Pt/CeO<sub>2</sub> shows catalytic activity for CO oxidation.

CO conversion over the Pt/CeO<sub>2</sub> catalysts increases rapidly at around 40°C (see Figure 9). As the temperature increases starting from room temperature (RT) in CO/air, the round Pt nanoparticles become partially faceted (see Figure 10). By comparing the shape of Pt nanoparticles under various conditions, it is possible to understand the mechanism for the shape change, and thereby the CO conversion rate which is dependent on temperature. It is proposed that the change in shape of the Pt nanoparticles is induced by the adsorption of CO molecules and O atoms.

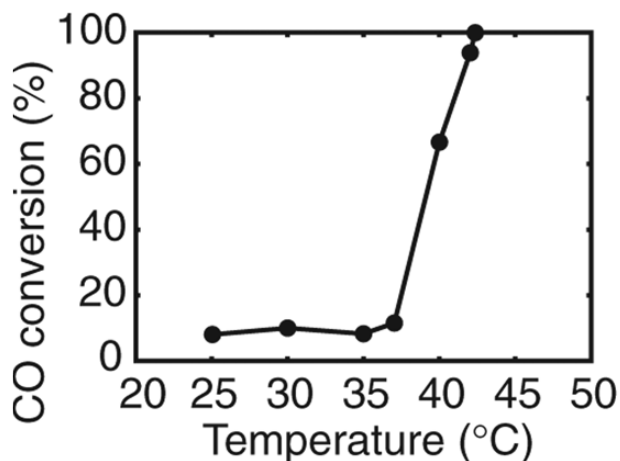


Figure 9. CO conversion over Pt/CeO<sub>2</sub> catalysts as a function of temperature.

Ref. H. Yoshida, et. al., *Applied Physics Express* 4 (2011) 065001. DOI: 10.1143/APEX.4.065001

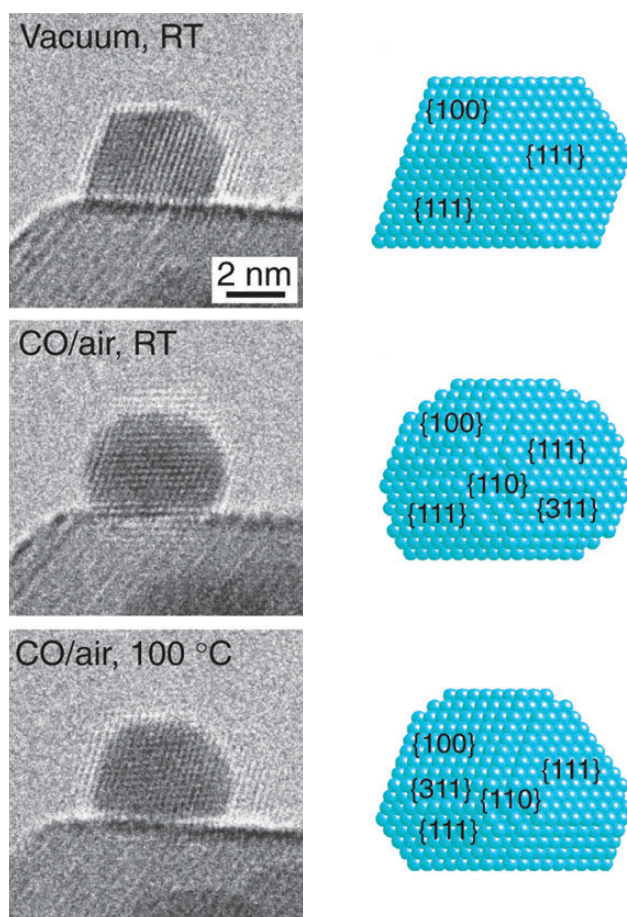


Figure 10. ETEM images of a Pt nanoparticle supported on CeO<sub>2</sub> in vacuum at RT and under realistic reaction conditions: at 1 mbar CO/air at RT (when the catalytic activity is low) and at 1 mbar CO/air at 100°C (when the catalytic activity is high). The corresponding three-dimensional atomic models of the Pt nanoparticle are based on the ETEM images and Wulff constructions.

Ref. H. Yoshida, et. al., *Applied Physics Express* 4 (2011) 065001. DOI: 10.1143/APEX.4.065001

**NOTE:** Certain gases may be not approved for use with the ETEM or their use may be restricted. Please contact Thermo Fisher Scientific for additional information on approved gases and our gas approval process.

## Catalytic low temperature CO oxidation: CO oxidation at room temperature—catalyst Au/CeO<sub>2</sub>

Bulk gold, as a noble metal, is rather unreactive, but gold nanoparticles behave much differently. Particularly surprising is the catalytic activity of gold clusters/nanoparticles supported on various metal oxides. For example, gold, when supported in the form of nanoparticles on crystalline metal oxides such as CeO<sub>2</sub>, is quite active towards the conversion of carbon monoxide to carbon dioxide, even at and below ambient temperatures (see Figure 11).

One crucial step of catalytic oxidation is the activation of the oxygen molecule, a cleavage of the O-O bond resulting in the formation of oxygen atoms. Another reaction step is the transfer of the oxygen atom to the carbon monoxide. To understand reaction mechanisms direct visualization of surface facets, surface reconstructions, atoms, and ideally of adsorbed gas molecules is vital (see Figures 12 & 13).

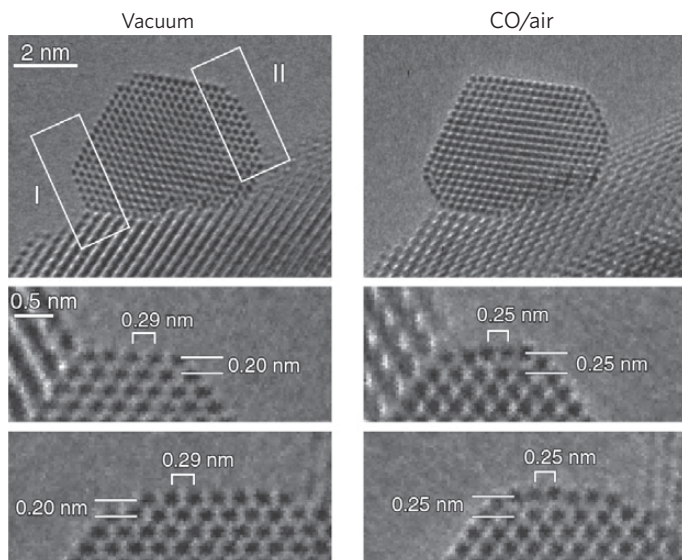


Figure 12. A gold nanoparticle supported on CeO<sub>2</sub> in a vacuum and in a reaction environment for CO oxidation (1 volume% CO in air gas mixture at 0.45 mbar at room temperature). Under catalytic conditions the gold nanoparticle exhibits Au {100}-hex reconstructed surface structures. Two {100} facets are present in the rectangular regions indicated by I and II. In vacuum, the distance between the topmost and the second topmost {100} surface layers of 0.20 nm was the same as the interplanar distance of the {200} planes in crystalline bulk gold. In the reaction environment, both the average distance of the adjoining Au atomic columns and the interplanar distance changed to 0.25 nm.

Ref. H. Yoshida, et. al., *Science* (2012) Vol. 335 no. 6066 317-319 DOI: 10.1126/science.1213194

Ref. T. Uchiyama, et. al., *Angew. Chem.* 2011, 123, 10339–10342, DOI: 10.1002/ange.201102487

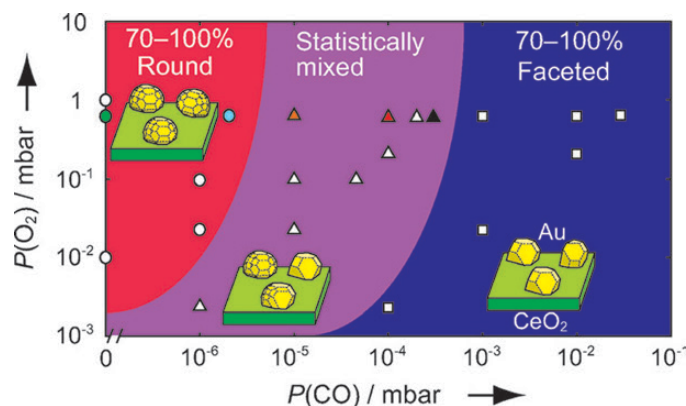


Figure 11. Morphology of gold nanoparticles supported on CeO<sub>2</sub>, as a function of the partial pressures of CO and O<sub>2</sub> in CO/air gaseous mixtures. The squares, triangles and circles represent faceted, statistically mixed, and rounded (dynamic multi-faceted) morphologies, respectively.

Ref. T. Uchiyama, et. al., *Angew. Chem.* 2011, 123, 10339–10342, DOI: 10.1002/ange.201102487

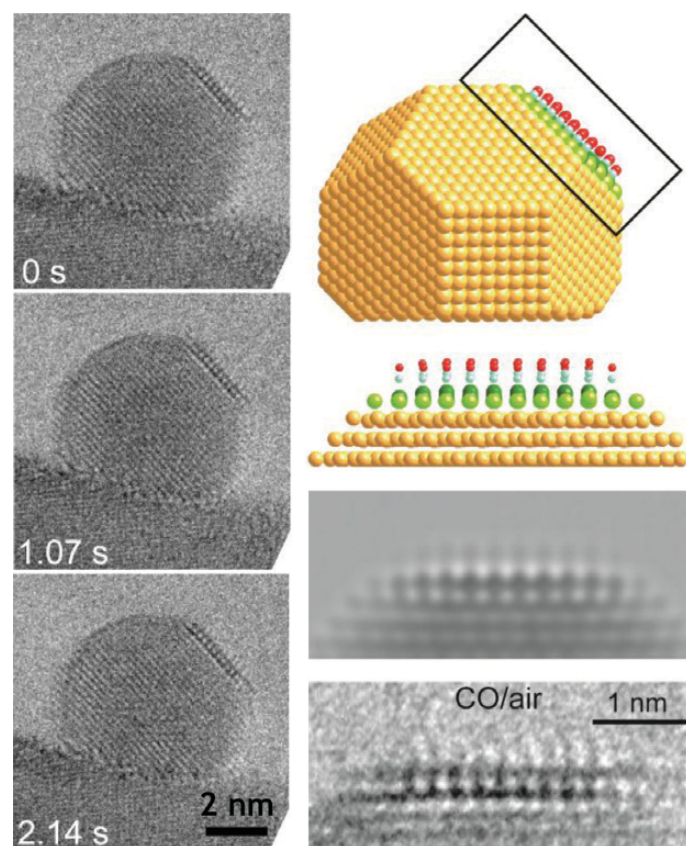


Figure 13. (Left) A gold nanoparticle supported on CeO<sub>2</sub> observed in reaction environment for CO oxidation (1 vol% CO in air gas mixture at 1 mbar at room temperature). An unusual image feature appeared on the upper-right part of the gold nanoparticle. (Right) Gold nanoparticle model with a Au {100}-hex reconstructed surface and adsorbed CO molecules for TEM image calculations. The rectangular area (box) is enlarged and shown just below the model. Comparison between the corresponding calculated TEM image and the experimentally observed image in CO/air confirm the presence of the Au {100}-hex reconstructed surface with adsorbed CO molecules.

Ref. H. Yoshida, et. al., *Science* (2012) Vol. 335 no. 6066 317-319 DOI: 10.1126/science.1213194

### Catalyst deactivation by sintering

Metal nanoparticles dispersed on a porous support material are used as efficient heterogeneous catalysts for diverse applications in energy conversion, chemical supply, and environmental protection.

However, the high-surface area of the nanoparticles is associated with an excess surface energy, so the nanoparticles represent a meta-stable solid state. Given sufficient thermal activation, the nanoparticles will sinter into larger particles. This coarsening causes an unwanted reduction in the metal surface area, which may affect the catalyst performance.

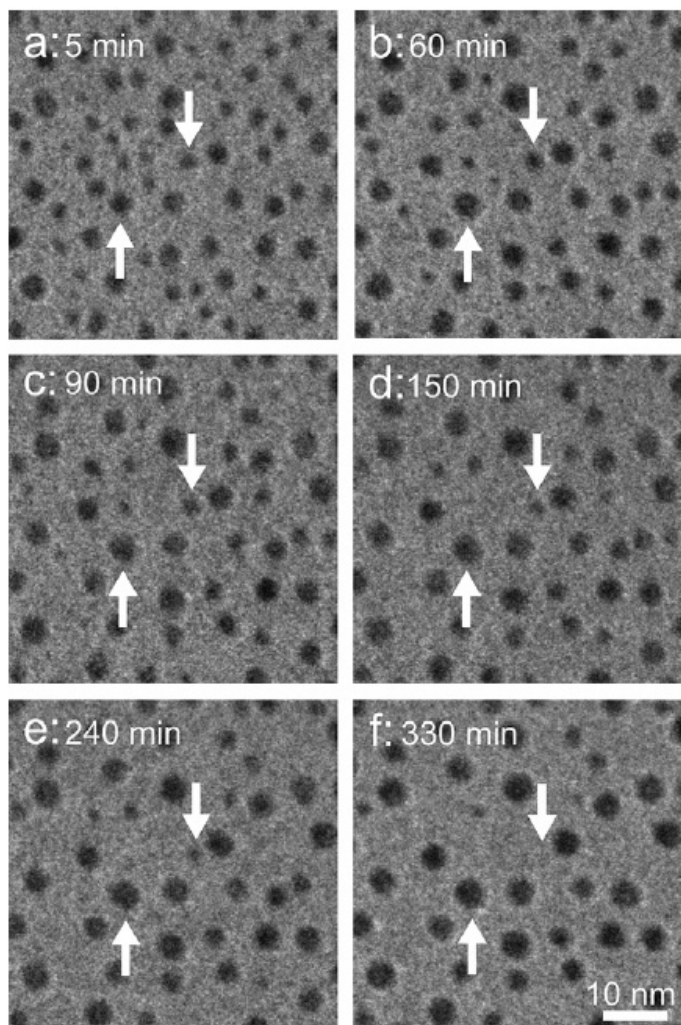


Figure 14. Observations of a Pt/SiO<sub>2</sub> model catalyst during exposure to 10 mbar air at 650°C to reveal unique mechanical and kinetic information on Pt nanoparticle ripening. This information enables a detailed comparison of the temporal evolution of the nanoparticle sizes with predictions made from different ripening models. Arrows indicate examples of a growing and of a decaying particle.

Ref. S. B. Simonsen, et. al., *Journal of Catalysis* 281 (2011) 147–155

Sintering on supported metal catalysts involves complex physical and chemical phenomena that make the understanding of the mechanisms of sintering difficult. At the microscopic level, the sintering is attributed to the transport of atomic species at surface of the nanoparticle or the support material (see Figures 14 & 15). The specific transport pathways for the atomic species are often considered to reflect the following generic sintering mechanisms:

- particle migration, in which the nanoparticles diffuse over the support and eventually coalesce with other nanoparticles, and;
- atom migration, in which atomic species are emitted from one nanoparticle, diffuse over the support, then attach to another nanoparticle.

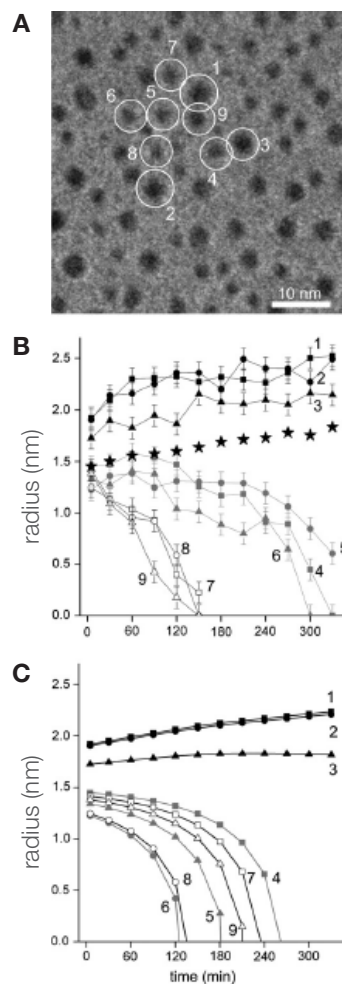


Figure 15. (A) An outline of the nine selected particles (white circles). (B) The particle radii for the particles 1–9 (A) as a function of time in the experiment. The mean radius for the whole TEM image (stars) is also presented. (C) Calculated time-dependent particle radii for the particles 1–9. The calculations used the interface-controlled ripening model based on the mean-field assumption.

Ref. S. B. Simonsen, et. al., *Journal of Catalysis* 281 (2011) 147–155

**NOTE:** Certain gases may be not approved for use with the ETEM or their use may be restricted. Please contact Thermo Fisher Scientific for additional information on approved gases and our gas approval process.

**Reduction–oxidation cycle: SOFC fuel cell anode**

A fuel cell is an energy conversion device that converts chemical energy from a fuel into electricity through an electrochemical reaction. The most commonly used fuel for this purpose is hydrogen (H<sub>2</sub>) gas, but hydrocarbons such as natural gas and alcohols (e.g. methanol) can also be used.

Solid oxide fuel cells (SOFC) are a class of fuel cell characterized by the use of a solid oxide material as the electrolyte. Advantages of SOFCs include flexibility of the used fuel, for example CO, H<sub>2</sub>, CH<sub>4</sub> (see Figure 16), delocalization of energy

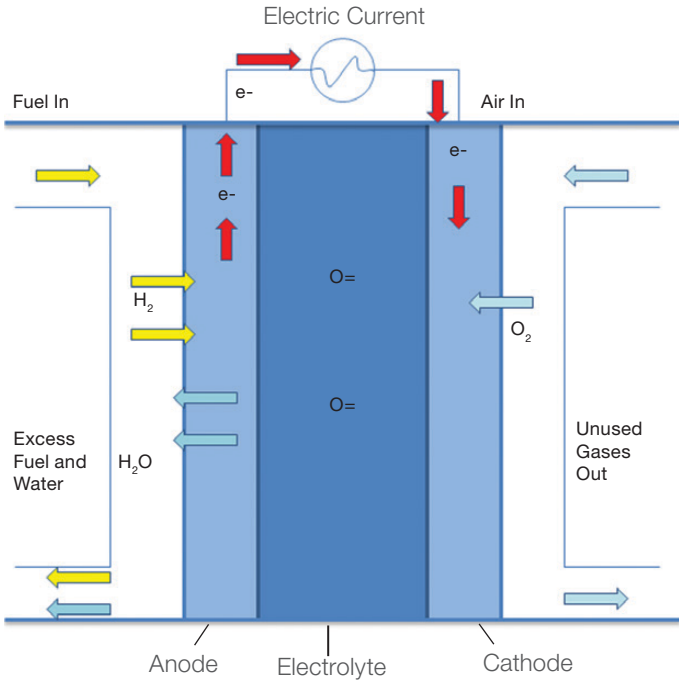


Figure 16. Reduction–oxidation cycle in a SOFC fuel cell anode.

production, reduction of pollutants such as mono-nitrogen oxides (NO<sub>x</sub>) and sulfur oxides (SO<sub>x</sub>). SOFCs also offer high efficiency, long-term stability, low emissions, and relatively low cost.

A standard solid oxide fuel cells design is based on an anode made of porous ceramic–metal composite yttria(Y<sub>2</sub>O<sub>3</sub>) stabilized zirconia (YSZ) and nickel (Ni) (see Figure 17).

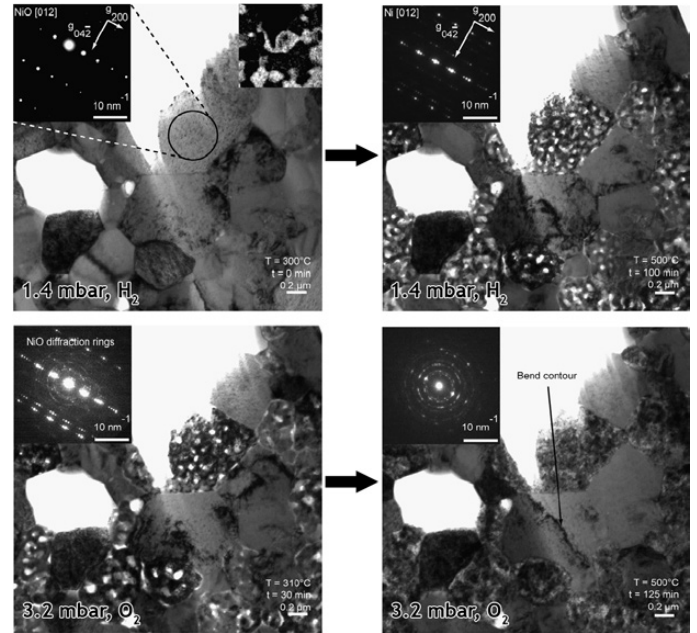


Figure 17. Understanding decreasing performance behaviors of the fuel cells due to structural changes on the anode. Evolution of the microstructure of the fuel cell anode made of yttria(Y<sub>2</sub>O<sub>3</sub>)-stabilized zirconia (YSZ) and nickel oxide (NiO) during *in situ* reduction and reoxidation. (Upper images) *In situ* reduction of a NiO–YSZ anode precursor in 1.4 mbar of H<sub>2</sub>. Nanoporosity is observed to form in the NiO grains to accommodate the volume shrinkage that results from the reduction of NiO to Ni. (Lower images) *In situ* reoxidation in 3.2 mbar O<sub>2</sub>. With increasing temperature, the nanoporosity that was created during *in situ* reduction is filled now by polycrystalline NiO. This occupies a larger volume than that of the as-sintered grains. Stress is observed in the YSZ phase, accumulating over successive redox cycles.

Ref. Q. Jeangros, et. al., Acta Materialia 58 (2010) 4578–4589

### Diesel automotive exhaust clean-up: soot oxidation

Carbonaceous nanoclusters, such as soot particles from the exhaust of diesel-driven engines, have an influence on our climate and also pose potential health risks. The awareness of soot abatement is increasing due to new environmental legislation for exhaust specifications.

Soot particles could be reduced either by optimizing the combustion inside the engine or by removing the carbonaceous particles from the gaseous exhaust stream.

These particles can be removed using a particulate filter. One approach to effectively regenerate the filters onboard is to functionalize the filters for catalytic oxidation of the deposited soot. Ceria( $\text{CeO}_2$ )-based materials are widely adopted for this purpose and have been the subject of several investigations (see Figures 18 & 19).

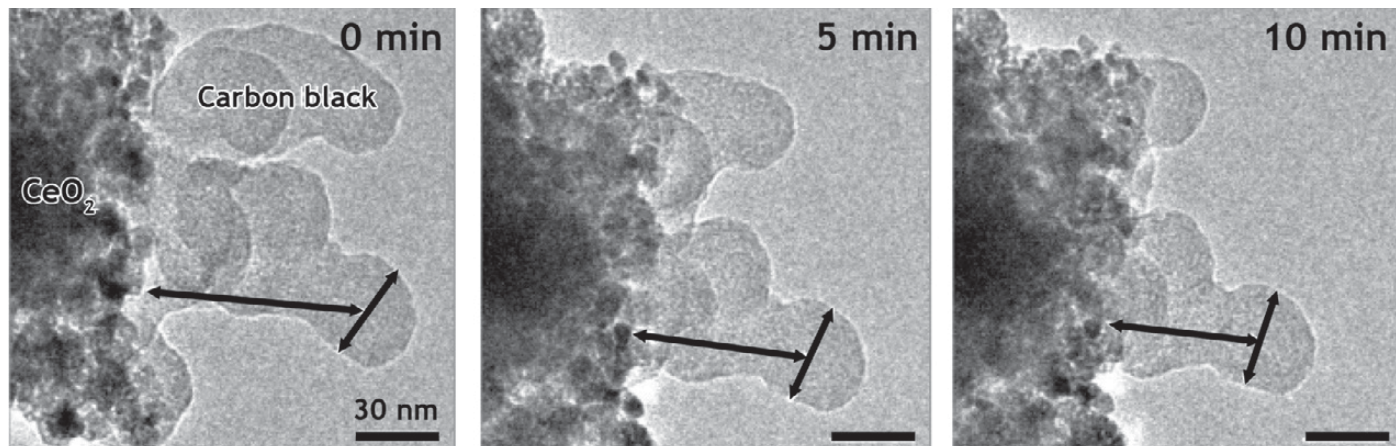


Figure 18. In situ study of the oxidation of an agglomerate of carbon black particles (diesel soot) attached to  $\text{CeO}_2$  by exposure to 2 mbar  $\text{O}_2$  at  $475^\circ\text{C}$ . The constant diameter of a carbon black particle, not the.

reduction of the carbon black- $\text{CeO}_2$  distance indicates that the oxidation occurs near the  $\text{CeO}_2$  surface.

Ref. S. B. Simonsen, et. al., *Journal of Catalysis* 255 (2008) 1-5

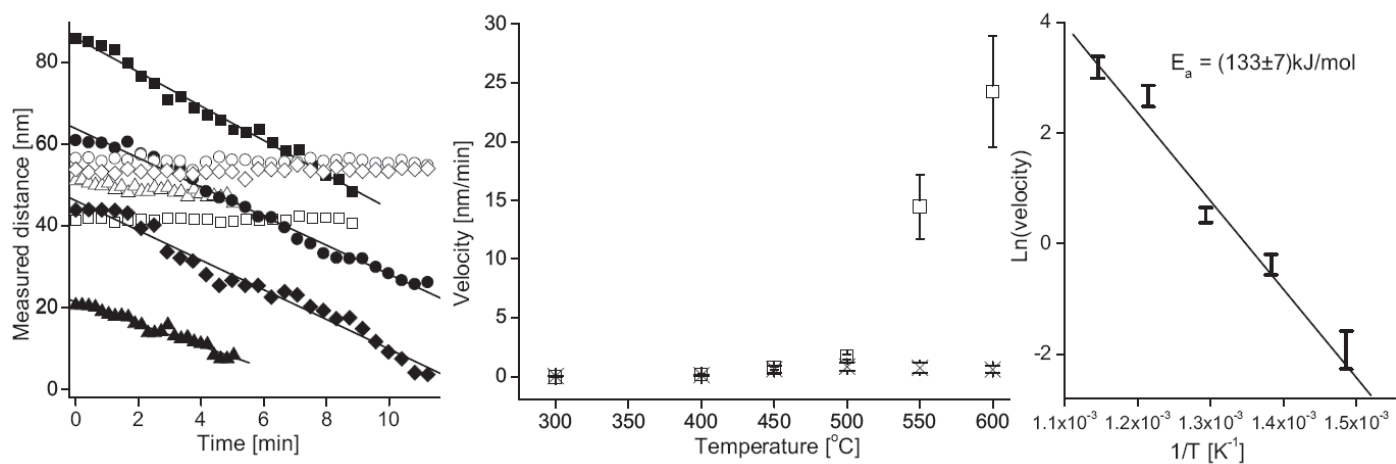
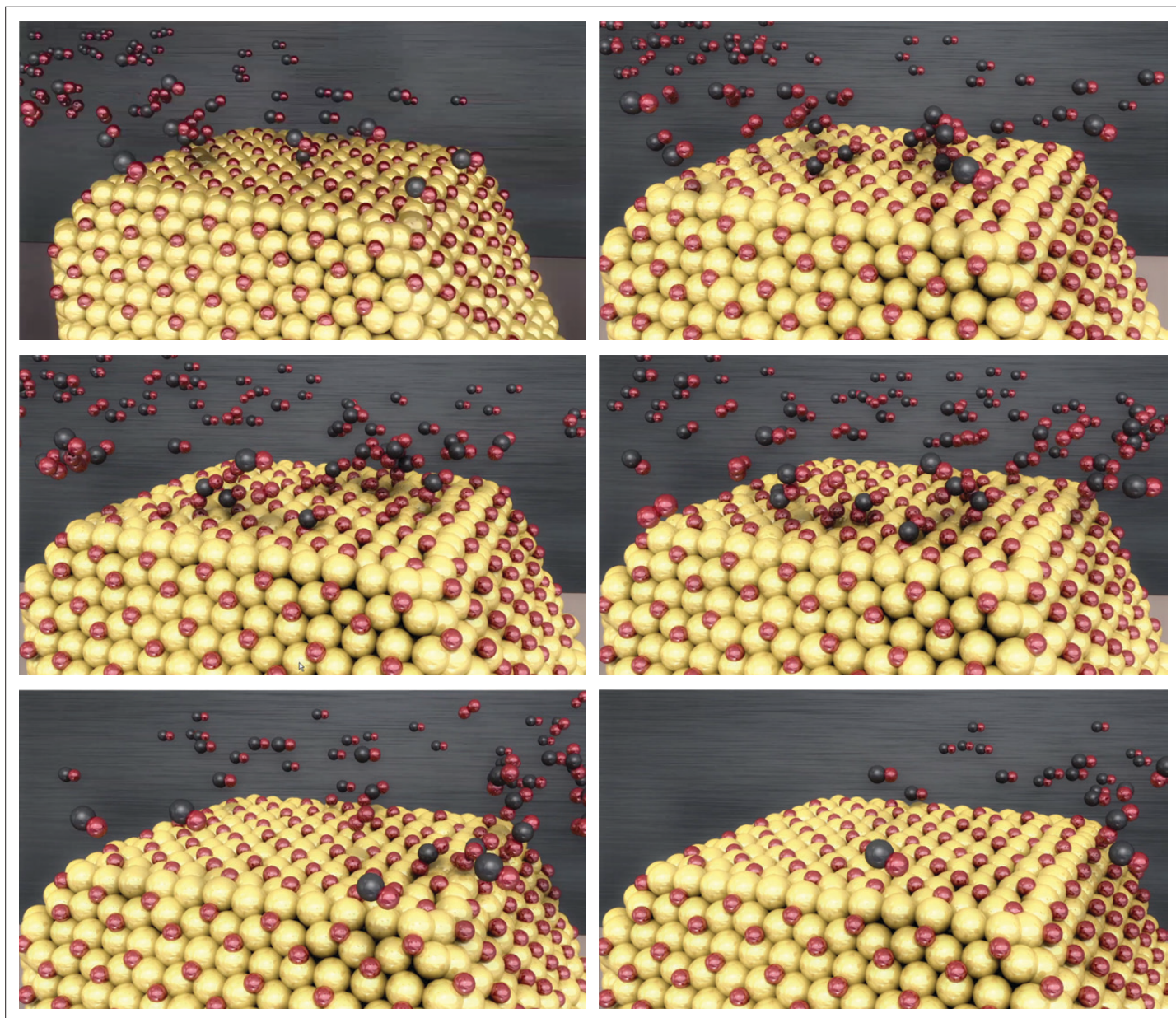


Figure 19. Several carbon black particles have been monitored and their diameter and their distance to the catalyst have been mapped out. (Left) Diameters (open symbols) of different carbon black particles and distances from the particle centers to the catalyst edge (filled symbols) as a function of time during exposure to 2 mbar  $\text{O}_2$  at  $475^\circ\text{C}$ . (Middle) The mean velocity of carbon black particles relative to  $\text{CeO}_2$  ( $\square$ ) and  $\text{Al}_2\text{O}_3$  ( $\times$ ) presented

for different temperatures. For each temperature, the average velocity and the standard deviation are obtained from observations of 10 particles in different agglomerates. (Right) Arrhenius plot of the mean velocities between carbon black particles relative to  $\text{CeO}_2$ .

Ref. S. B. Simonsen, et. al., *Journal of Catalysis* 255 (2008) 1-5

**NOTE:** Certain gases may be not approved for use with the ETEM or their use may be restricted. Please contact Thermo Fisher Scientific for additional information on approved gases and our gas approval process.



Find out more at [thermofisher.com/EM-Sales](https://thermofisher.com/EM-Sales)

**ThermoFisher**  
SCIENTIFIC